INTERACTION OF LASER RADIATION WITH MATTER. LASER PLASMA PACS numbers: 52.50.Jm; 52.25.Nr
DOI: 10.1070/QE2000v030n10ABEH001830

Effect of the nonuniformities of a diagnostic laser beam on the interpretation of experiments on turbulent mixing

S A Bel'kov, O A Vinokurov, S G Garanin, G V Dolgoleva, G G Kochemasov, E I Mitrofanov, N A Suslov

Abstract. The results of experiments on the turbulent mixing in the acceleration of Si/Al/Au and Si/Al/Mg three-layer targets on the ISKRA-4 high-power laser facility were analysed on the basis of calculations. It was shown that the onset of the line emission of helium-like aluminium upon irradiation of the rear side (Au or Mg) of the target with a diagnostic laser beam can be determined not only by the degree of turbulent mixing of Al and Au (Mg), but also by the 'hot spots' in the lateral structure of the diagnostic beam.

1 . Introduction

Turbulent mixing, which develops at the interface of light and heavy material layers when they are accelerated by laser or x-ray radiation, is the key problem for laser fusion because it can have a significant effect on the stability of operation of fusion targets, their energy efficiency, etc. This arouses interest in turbulent mixing studies, which are pursued on high-power laser facilities [1 – 4].

Two principal approaches to the study of hydrodynamic instabilities are presently known. The first involves investigations of the linear or weakly nonlinear stages of the Rayleigh – Taylor instability of single-mode perturbations [1]. In these experiments, one detects the time variation of the initial perturbations introduced in a controllable manner on the surface or plane, cylindrical, or spherical target.

The second approach is aimed at studying the strongly nonlinear stage of hydrodynamic instabilities, which is characterised by the interaction of a large number perturbation modes, and it is not until this stage that we are dealing with turbulent mixing [2 – 4]. In these experiments, laser radiation is used to accelerate targets composed of different-density material layers at whose interfaces the conditions for the development of gas-dynamic instability are realised. The diagnostics of mixing involves measurements of the time delay of the emission of spectral lines of different layer materials upon backside irradiation of the accelerated target by a special diagnostic laser beam.

S A Bel'kov, O A Vinokurov, S G Garanin, G V Dolgoleva, G G Kochemasov, E I Mitrofanov, N A Suslov All-Russian Federal Nuclear Centre, All-Russian Research Institute of Experimental Physics, prosp. Mira 37, 607190 Sarov, Nizhny Novgorod oblast, Russia

Received 22 February 2000; revision received 13 June 2000
Kvantovaya Elektronika **30** (10) 884 – 888(2000)
Translated by E N Ragozin

Here, we performed a simulation-assisted analysis of experiments [3, 4] on the investigation of turbulent mixing performed on the ISKRA-4 facility [5] and considered one of the possible reasons for the discrepancy between the experimental and calculated data observed in Refs [3, 4].

In the experiments under discussion, an study was made of the turbulent mixing developing at the interface between thin Al and Au layers during three-layer (Si/Al/Au) target acceleration. The target was composed of a silicon layer with a density $\rho_{Si} = 2.3$ g cm^{-3} of thickness $\Delta_{Si} \approx 5$ μm, an aluminium layer ($\rho_{Al} = 2.7$ g cm^{-3} and $\Delta_{Al} \approx 2$ μm), and a gold layer ($\rho_{Au} = 19.3$ g cm^{-3}) ranging in thickness Δ_{Au} from 0.05 to 0.4 μm. The target was accelerated by a driving laser pulse with an intensity of $(4-7)\times10^{13}$ W cm^{-2}, a pulse duration $\tau_{0.5} \sim 0.3 - 0.1$ ns, and a wavelength $\lambda = 0.657$ μm, which irradiated the target on the Si side. The prerequisites for the Rayleigh – Taylor instability development are realised at the Al/Au interface, which results in turbulent mixing.

The occurrence of turbulent mixing in Refs [3, 4] was deduced from the comparison of the experimental time delay between the continuous x-ray emission of Au and the He_α line emission of Al with the calculated time of heating of the Au layer by the thermal wave excited by a special diagnostic laser with an intensity of $(1-4)\times10^{13}$ W cm^{-2}. The latter irradiated the target on the Au layer side. In order for the He_α line emission of Al to be observable against the continuous background, a strongly nonequilibrium plasma should be produced. To accomplish this in diagnostics, advantage is taken of a laser pulse to produce an electron thermal wave, which heats the Au and Al layers. The heat transfer is accomplished primarily due to the electron heat transfer rather than the radiative one. For the mixing process to have time to develop, the diagnostic laser beam should be delayed by $\Delta t \sim 0.9$ ns relative to the driving one.

These experiments were analysed employing the SND-TUR one-dimensional radiative gas dynamic code [6]. The following physical processes were included in the calculations: the absorption of laser radiation due to inverse bremsstrahlung, gas dynamics, electron and ion thermal conduction, the electron – ion relaxation, the nonequilibrium spectral diffusion of x-ray radiation, the ionisation kinetics of a multiply charged multicomponent plasma in the average-ion approximation, and the turbulent mixing in the context of the Nikiforov model. The numerical analysis [3] showed that the time delay Δt_{Au-Al} between the continuous x-ray emission of Au and the He_α line emission of Al for Si/Al/Au targets with a thickness of the gold layer $\Delta_{Au} = 0.3$ μm is 0.1 ns, which should be reliably recorded by the streak camera with a time resolution of better than

0.05 ns. However, a simultaneous commencement of both the continuous x-ray emission of Au and the line emission of helium-like Al was observed experimentally for all thicknesses of the gold layer (0.05 – 0.4 μm).

In [4], the results of similar experiments on the acceleration of three-layer Si/Al/Mg targets (the density of magnesium is $\rho_{Mg} = 1.76$ g cm^{-3}) are reported. The difference between the two targets is that the Al/Mg interface is stable and the turbulent mixing should not develop. Figs 1 and 2 show the experimental and calculated (the SNDP [7] code was employed to carry out one-dimensional simulations with inclusion of the same physical processes as in the case of SND-TUR-assisted simulations, with the exception of turbulent mixing) time dependences of the He_α Al and He_β Mg line emission from the rear side (on the Mg side) of the Si/Al/Mg target with a Mg layer thickness of 0.8 μm. The calculated delay between the line emission of Mg and Al is $\Delta t_{Mg-Al} \approx 0.68$ ns, which is well above the experimental one equal to ~ 0.3 ns.

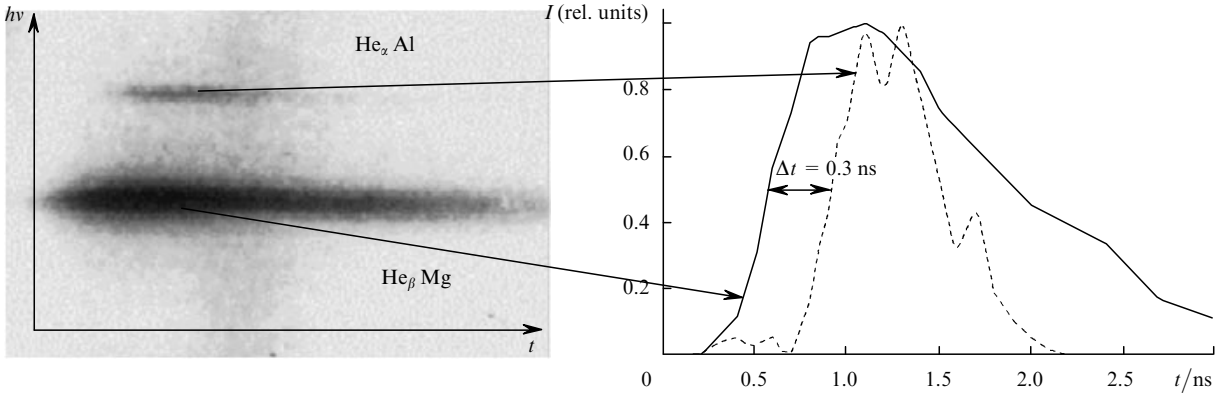

Figure 1. Experimental time dependences of the He_α Al and He_β Mg line emission from the rear side of the target [4].

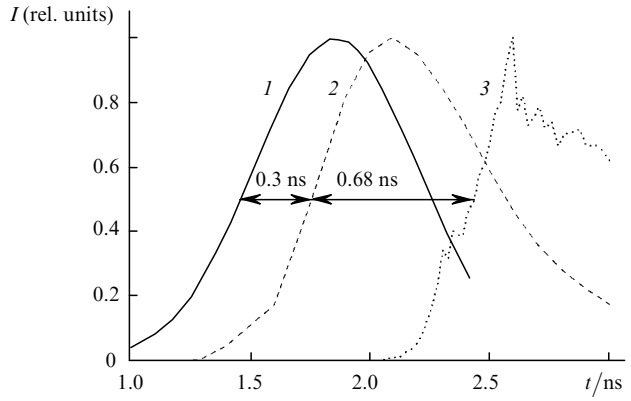

Figure 2. Calculated time dependences of the diagnostic laser pulse (*1*) and the He_β Mg (*2*) and He_α Al (*3*) line emission from the rear side of the target.

One of the reasons why the results of one-dimensional calculations and experiments are different may be the nonuniformity of the intensity distribution of the diagnostic laser beam at the target surface, which is responsible for an 'earlier' burning through of Au or Mg compared to the one-dimensional simulations. A random phase plate (RPP) was employed to smooth out large-scale nonuniformities of the laser beams (driving and diagnostic) in Refs [3, 4]. As is well known [8], using an RPP results in the formation of a quasistationary speckle intensity distribution of laser radiation, which has a Gaussian-like envelope with a small-scale intensity modulation, at the point of target location (in the far-field region). The modulation amplitude can be as high as 100% while the spatial speckle ('hot' spot) dimension r_0 is primarily determined by the diffraction-limited beam divergence, $r_0 \sim \lambda F/D$, where λ is the laser radiation wavelength, F is the focal length of the lens, and D is the diameter of the laser beam. In the experiments under discussion, $r_0 \approx 10 - 12$ μm.

An initial estimate of the effect of nonuniformity of the intensity distribution of the diagnostic beam will be made in the so-called sector approximation, as applied to the experiments of Ref. [4] with Si/Al/Mg targets. For this purpose, it will be assumed that the intensity of Mg (or Al) line emission depends only on the local intensity of laser radiation in the diagnostic beam.

To take into account the real nonuniformity of laser radiation, we introduce the intensity distribution of the energy of the diagnostic beam $dE(I)/dI$. Then, the intensity of Mg (or Al) line emission can be represented as

$$P_{Mg(Al)}(t) = \int_0^\infty I^0_{Mg(Al)}(I,t)\,\frac{1}{I}\,\frac{dE}{dI}\,dI, \qquad (1)$$

where $I^0_{Mg(Al)}(I,t)$ is the intensity of Mg (or Al) line emission as a function of the intensity of the diagnostic beam I obtained from one-dimensional calculations by the SNDP code.

A consideration of the calculated dependences I^0_{Mg} and I^0_{Al} shows that varying the diagnostic beam intensity from 10^{13} to 10^{14} W cm^{-2} reduces the time delay Δt_{Mg-Al} from ~ 0.7 to ~ 0.4 ns. Integration of expression (1) with the distribution function dE/dI derived on the basis of the distribution of laser radiation intensity at the target surface obtained experimentally in Ref. [4] indicates that an earlier magnesium burn-through in the higher-intensity region results in a reduction (in comparison with the calculation for an average intensity, $\Delta t_{Mg-Al} \approx 0.68$ ns) of the time delay to $\Delta t_{Mg-Al} \approx 0.41$ ns (see Fig. 4). This value is in a much better agreement with the experimental value $\Delta t_{Mg-Al} \approx 0.3$ ns.

However, the sector approximation does not take into account two-dimensional effects which may, in principle,

smooth out the intensity nonuniformities in the plasma corona and lower the rate of Mg 'burn-through' the hot spots. In particular, the electron thermal conduction can have a significant effect on the nonuniformity of the thermal wave in the ablation region.

A gas-dynamic flow description that is more adequate for the experimental conditions can be obtained on the basis of two-dimensional gas-dynamic simulations, which we conducted employing the two-dimensional complex MIMOZA-ND code [9]. These simulations took into account the same physical processes as the one-dimensional simulations by the SNDP code.

Fig. 3 shows the geometry of the two-dimensional calculations, which were performed assuming that the symmetry of the problem is cylindrical. A multilayer Si/Al/Mg target was irradiated on the Si side by the laterally uniform driving laser pulse $I_p(t)$, which accelerated the target. The temporal shape of the driving pulse approximated the experimental one and was prescribed as

$$I_p(t) = I_{pm}\left\{0.34\exp\left[-\left(\frac{t-t^*}{\tau_0}\right)^2\right] + 0.39\exp\left[-\left(\frac{t-t^*-\Delta t}{\tau_0}\right)^2\right] + 0.12\exp\left[-\left(\frac{t-t^*-2\Delta t}{\tau_0}\right)^2\right]\right\},$$

where $\tau_0 = 0.48$ ns, $I_{pm} = 8\times10^{13}$ W cm^{-2}, $\Delta t = 0.6$ ns.

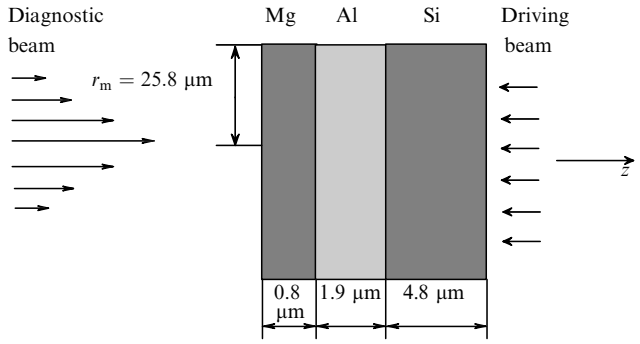

Figure 3. Two-dimensional simulation geometry.

Because the intensity distribution of the diagnostic beam over the target surface was rather complex in form [4], we simulated only a small fragment of the diagnostic beam $I_d(r, t)$ in the neighbourhood of a bright spot with a characteristic dimension r_0 selected on the basis of the known lateral intensity distribution [4]:

$$I_d(r,t) = I_{dm}\exp\left[-\left(\frac{r}{r_0}\right)^2\right]\exp\left[-\left(\frac{t-t^*-\Delta t_{pd}}{\tau_0}\right)^2\right], \quad (2)$$

where $I_{dm} = 4.5\times10^{13}$ W cm^{-2}, $r_0 = 12$ μm, and $\Delta t_{pd} = 0.86$ ns.

The lateral dimension of the computation range, $r_m = 25.8$ μm, and the intensity at the spot centre I_{dm} were determined from the condition that the ratio between the intensities at the beam centre and at the edge is $I_d(0,t)/I_d(r_m,t) = 100$ while the intensity averaged over the beam cross section coincides with the peak intensity of the diagnostic pulse in the one-dimensional calculation [4]:

$$\frac{1}{\pi r_m^2}\int_0^{r_m} I_{dm}\exp\left[-\left(\frac{r}{r_0}\right)^2\right]2\pi r\,dr = I_{dm}^0 = 9.7\times10^{12}\ \text{W cm}^{-2}.$$

The gas dynamics was calculated employing a Lagrangian-Eulerian technique. The computational mesh had 100 cells in the longitudinal direction (along the z-axis aligned with the direction of laser beam propagation) and 40 cells in the lateral direction. In this case, the computation in the longitudinal direction was effected on a purely Lagrangian mesh. The transfer of x-ray radiation was calculated in the approximation of nonequilibrium spectral diffusion on a mesh comprising six groups in the photon energy range $h\nu = 0-0.7-1.3-1.5-1.8-2.0-3.0$ keV. The equation of state, the electron and ion heat conductivity coefficients, the electron-ion relaxation rate, the laser-radiation absorption coefficient, and also the nonequilibrium coefficients of absorption and emission of x-ray plasma radiation were calculated in the approximation of an average-ion ionisation kinetics [10].

The intensity of Al and Mg line emission was calculated in the course of post-processor treatment of the two-dimensional distributions of density, temperature, and average population densities of ion levels, which were used to reconstruct the densities of excited helium-like ions at a given plasma point in space at a given point in time. The known excited ion densities were used to calculate the emission intensities of the corresponding lines. To find the line intensity at the target surface, the stationary line-transfer equation was then solved along the z-axis with given density and temperature profiles. The temporal line shape was determined by integrating the line intensity distribution over the target surface in the lateral cross section.

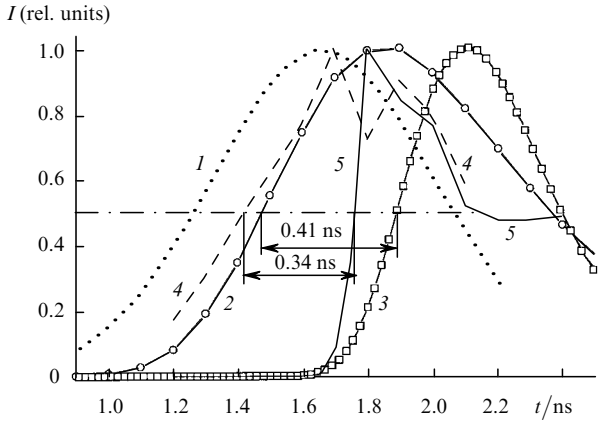

Figure 4. Calculated time dependences of the diagnostic laser beam (*1*) and the emission of Mg (*2*), He_α Al (*3*), Mg (*4*), and He_α Al (*5*) from the rear side of the target. Dependences *2* and *3* were calculated in the sector approximation by the SNDP code; the dependences *4* and *5* represent the two-dimensional calculation by the MIMOZA code.

Fig. 4 presents the calculated time dependences of the He_α Al and He_β Mg line emission from the rear side of the target. Also shown for comparison are the relevant dependences obtained in the sector approximation. Referring to

Fig. 4, the calculated (by the MIMOZA code) delay between the line emission of Mg and Al is 0.34 ns, which is close to the experimental one (0.3 ns).

In addition to the above assignment of the spatial nonuniform intensity distribution in the hot spot of the diagnostic beam in the form of expression (2), we performed simulations with a spatial intensity distribution in the spot in prescribed by the formula

$$I_{\mathrm{d}}(x) = I_{\mathrm{dm}} \cos\left(\frac{\pi}{2}\frac{x}{r_0}\right).$$

As shown by these calculations, the lateral nonuniformity of the electron temperature at the Mg – Al interface is practically nonexistent. This is ascribed to the fact that the maximum-to-average intensity ratio in this case was smaller than in the case of equation (2) [this ratio is equal to two for a cosine distribution and to approximately 4.6 for a distribution of the form (2)].

Therefore, the calculations conducted suggest that, to apply the method of investigation of turbulent mixing outlined in Refs [3, 4], a diagnostic laser beam should be used in which the maximum-to-average intensity ratio is no greater than 2 – 3. Different methods for smoothing can be used to obtain the diagnostic beam with an intensity distribution of appropriate quality, such as smoothing by spectral dispersion (SSD) [11] or the method of a plasma phase plate [12].

The significance of the effect of the hot spots in the intensity distribution of the diagnostic laser beam on the x-ray radiation from the rear side of the target is confirmed by the target images obtained with a pinhole camera in experiments staged on the ISKRA-4 facility. A comparison of the pinhole-camera images of the rear side of the target given in Fig. 5 shows that the x-ray radiation intensity distribution is, for experiments where the rear side of the target bears a gold layer, strongly nonuniform and reflects the small-scale lateral nonuniformities of the diagnostic beam. The emission is practically uniform for experiments on the targets with a rear-side magnesium layer.

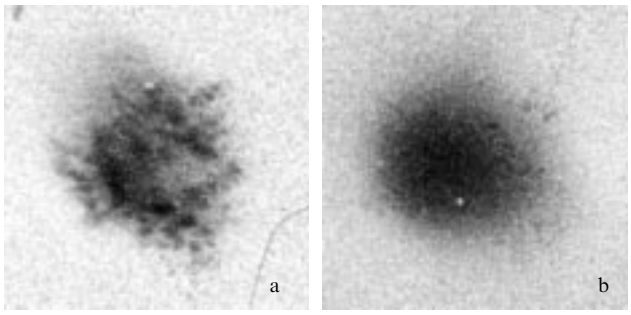

Figure 5. Pinhole-camera images of the target on Au (a) and Mg (b) layer side recorded in experiments on the ISKRA-4 facility.

One of the reasons why the observed images are so much different may be the difference in the electron heat conductivity coefficients of Au and Mg. The electron heat conductivity coefficient is inversely proportional to the average plasma charge, which is significantly higher for a gold plasma than for a magnesium plasma. In this connection the smoothing of the temperature nonuniformity in the laser corona, which arises owing a nonuniformity of the laser beam, by way of the lateral heat transfer mechanism will in the former case perform worse than in the latter.

To shed light on the role played by the electron heat transfer in the formation of nonuniform x-ray target emission, a two-dimensional simulation was performed employing the MIMOZA-ND code. The formulation of the problem was similar to that described above, except that the Mg layer was replaced with an Au layer 0.2 μm in thickness. Fig. 6 shows the calculated distributions of the Mg and Au plasma emission intensities at the point in time $t = 1.8$ ns for the 0.7 – 1.3 keV x-ray photon energy range. One can see that the emission intensity of the gold plasma at centre of the laser spot is several orders of magnitude stronger than that at the edge while the nonuniformity of the emission intensity for the magnesium plasma is much weaker. As evidenced by the simulations, this is uniquely related to the nonuniformity of the temperature.

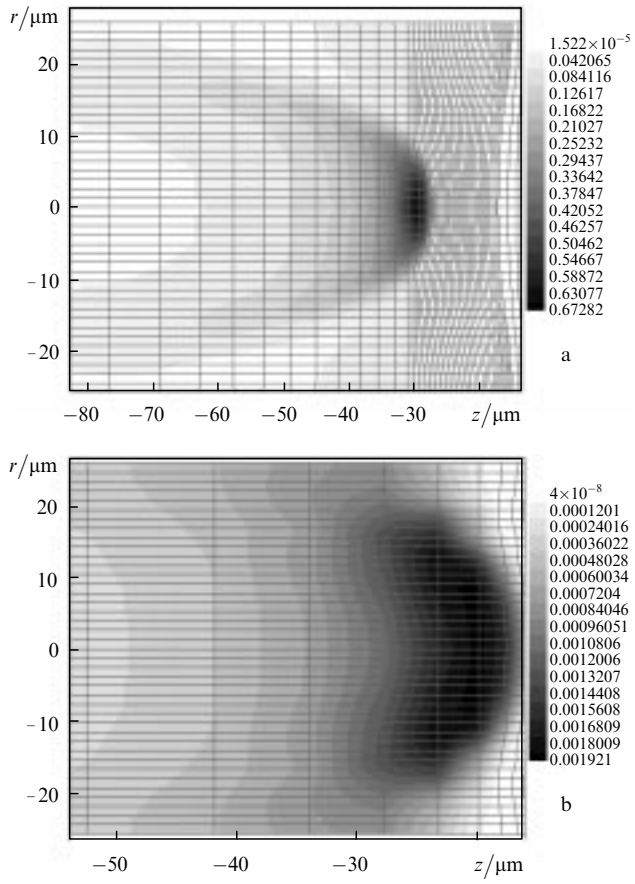

Figure 6. Calculated two-dimensional distributions of the emission intensity and gas dynamic meshes in Au (a) and Mg (b) at the point in time $t = 1.8$ ns.

The simulation-assisted theoretical analysis involving one-dimensional sector calculations by the SNDP code and two-dimensional calculations by the MIMOZA code suggests that the interpretation of the measured time delay of the line emission of different material layers, which originates when the rear side of the accelerated three-layer target is irradiated by a diagnostic laser pulse, essentially depends on the character and the degree of nonuniformity of the spatial intensity distribution in the diagnostic laser beam.

In particular, the existence of small high-intensity spots can be responsible for a reduction (in comparison with a one-dimensional calculation) of the time delay between the onset of the He_β Mg and He_α Al line emission in experiments on the acceleration of stable three-layer Si/Al/Mg targets, when the turbulent mixing at the aluminium – magnesium interface does not occur. In this case, the backside pinhole-camera images recorded in the intrinsic continuous x-ray plasma radiation show, for low-Z materials, no small-scale nonuniformities in the emission intensity distribution owing to a strong temperature equalisation in the laser corona effected by the lateral electron thermal conduction.

In the case of experiments with unstable targets of the Si/Al/Au composition, when the turbulent mixing develops at the aluminium – gold interface, the existence of hot spots hinders the comparison of experimental data with those obtained by the simulations in the context of one-dimensional models of turbulent mixing. These hot spots are clearly defined in the pinhole-camera backside target images due to a significantly weaker electron heat conductivity in high-Z targets.

Therefore, it may be concluded that to measure the width of the mixing region from the aluminium line emission in experiments on the acceleration of multilayer targets, particular emphasis should be placed on the techniques of smoothing out the diagnostic beam. Furthermore, the consequences of two-dimensional effects for the formation of line emission should be taken into account.

Acknowledgements. This work was supported in part by the Russian Foundation for Basic Research, Grant Nos 96-15-96508 and 96-01-00046.

References

1. Chrien R E, Barnes C W, Beck J B, et al., in *Advances in Laser Interaction with Matter and Inertial Fusion* (Singapore: World Scientific, 1997) p. 30
2. Holstein P A, Meyer B, Rostaing M, et al. *Compte Rendu Acad. Sci. Paris* **307** 211 (1988)
3. Andronov V A, Bel'kov S A, Bessarab A V, et al. *Zh. Eksp. Teor. Fiz*. **111** 882 (1997) [*J. Exp. Theor. Phys*. **84** (3) 485 (1997)]
4. Bel'kov S A, Andronov V A, Bessarab A V, et al., in *Proceedings of the Sixth International Workshop on the Physics of Compressible Turbulent Mixing, Marseille*, 1997, p. 13
5. Gasheev A S, Zaretskii A I, Kirillov G A, et al. *Pis'ma Zh. Eksp. Teor. Fiz.* **7** 1368 (1981)
6. Andronov V A, Bel'kov S A, Dolgoleva G V, et al. *Vopr. At. Nauki i Tekh. Ser. Matem. Model. Fiz. Protsessov* (3) 1 (1997)
7. Bel'kov S A, Dolgoleva G V *Vopr. At. Nauki i Tekh. Ser. Matem. Model. Fiz. Protsessov* (1) 59 (1992)
8. Kato Y, Mima K, Myuga N, et al. *Phys. Rev. Lett*. **53** 1057 (1984)
9. Afanas'eva E A, Vinokurov O A, Sofronov I D, et al., in *Konstruirovanie Algoritmov i Reshenie Zadach Matematicheskoi Fiziki* (Construction of Algorithms and Solution of the Problems of Mathematical Physics) (Moscow: Keldysh Institute of Applied Mathematics, USSR Academy of Sciences, 1989) p. 277
10. Bel'kov S A, Gasparyan P D, Kochubei Yu K, Mitrofanov E I *Zh. Eksp. Teor. Fiz.* **111** *496 (1997)* [*J. Exp. Theor. Phys.* **84** *(2) 272 (1997)]*
11. Skupsky S, Short R W, Kessler T, Craxton R S, Letzring S, Soures J M *J. Appl. Phys*. **66** 3456 (1989)
12. Derkach V N, Bondarenko S V, Garanin S G, et al., in *Technical Programme and Book of Abstracts of XXV ECLIM* (Formia, Italy, 1998, MO/P/3)